Geosynthetic Soil Reinforcement Testing Procedures

S. C. Jonathan Cheng, editor

ASTM

STP 1190

STP 1190

Geosynthetic Soil Reinforcement Testing Procedures

S. C. Jonathan Cheng, editor

ASTM Publication Code Number (PCN)
04-011900-38

ASTM
1916 Race Street
Philadelphia, PA 19103

Library of Congress Cataloging-in-Publication Data

Geosynthetic soil reinforcement testing procedures / S.C. Jonathan Cheng, editor.
(STP ; 1190)
Includes bibliographical references and index.
ISBN 0-8031-1885-6
1. Soil stabilization--Testing. 2. Geosynthetics--Testing. I. Cheng, S. C. Jonathan (Shi-Chieh Jonathan) II. Series: ASTM special technical publication ; 1190.
TA710.5.G44 1993
624.1'51363--dc20 93-8893
CIP

Peer Review Policy

Each paper published in this volume was evaluated by three peer reviewers. The authors addressed all of the reviewers' comments to the satisfaction of both the technical editor(s) and the ASTM Committee on Publications.

To make technical information available as quickly as possible, the peer-reviewed papers in this publication were printed "camera-ready," as submitted by the authors.

The quality of the papers in this publication reflects not only the obvious efforts of the authors and the technical editor(s), but also the work of these peer reviewers. The ASTM Committee on Publications acknowledges with appreciation their dedication and contribution to time and effort on behalf of ASTM.

Printed in Fredericksburg, VA
August 1993

Foreword

This publication, *Geosynthetic Soil Reinforcement Testing Procedures,* contains papers presented at the symposium of the same name, held in San Antonio, TX on 19 Jan. 1993. The symposium was sponsored by ASTM Committee D-35 on Geosynthetics. S. C. Jonathan Cheng of Drexel University in Philadelphia, PA, presided as symposium chairman and is the editor of the resulting publication.

Overview

This ASTM symposium provides a forum for presentation of state-of-the-art technologies and new developments in geosynthetic soil reinforcement testing. The topics addressed include mechanical and durability properties with respect to the reinforcement function of geosynthetics, analysis of reinforcement testing results, and evaluation of testing results in relation to design. This symposium was also a result of an ASTM Committee D-35 seminar held in June 1991, concerning the same topic of geosynthetic soil reinforcement testing.

Since the use of geosynthetics in reinforcement applications is rapidly increasing, there is a need to institute a rational technical base for an understanding of the performance of geosynthetics in reinforcement applications. The corner stone of this technical base is the timely development of standardizing test methods, that is the charter of Committee D-35 on Geosynthetics. Although much progress has been witnessed as more testing methods are made available through ASTM processes, there is a significant lag betwen the state-of-the-art and present standardized test methods. This symposium attempts to provide a bridge between this time gap.

The organization of this Special Technical Publication (STP) is as follows:

(1) Papers associated with either new testing equipment/procedures, or testing procedures for new reinforcement applications are included. These papers provide direction in the development of standard testing methods (papers 1 through 5).
(2) Papers evaluating procedures of testing methods that are standardized or widely used are also included. The discussions are focused on those factors that influence test results (papers 6 through 10).
(3) The next section of papers are concerned with the analysis of testing results in relation to design. In terms of standard practice, this is an area of need within ASTM (papers 11 through 14).
(4) Finally, papers associated with the durability issue of geosynthetic reinforcement applications conclude this STP (papers 15 through 17).

All of the papers in this STP went through a rigorous review process. I would like to extend my most sincere appreciation to the authors for their enthusiastic participation and to the reviewers for their professional critiques. My work as editor of this publication has been very rewarding, but the credit must go to the authors and reviewers. In addition, I would like to thank the administrative support group from ASTM, especially Mrs. Dorothy Savini, Ms. Rita Hippensteel, and Mrs. Therese Pravitz.

This symposium is a step towards fully understanding the technical performance of geosynthetics. It is my most sincere hope that it will catalyze further research work and technical advancement.

Shi-Chieh Cheng

Drexel University, Philadelphia, PA; symposium chairman and editor.

Contents

Andrew J. Whittle[1], Douglas G. Larson[1], John T. Germaine[1] and Mauricio Abramento[1]

A NEW DEVICE FOR EVALUATING LOAD-TRANSFER IN GEOSYNTHETIC REINFORCED SOILS

REFERENCE: Whittle, A.J., Larson, D.G., Germaine, J.T. and Abramento, M. **"A NEW DEVICE FOR EVALUATING LOAD-TRANSFER IN GEOSYNTHETIC REINFORCED SOILS,"** Geosynthetic Soil Reinforcement Testing Procedures, ASTM STP 1190, S.C. Jonathan Cheng, Ed., American Society for Testing and Materials, Philadelphia, 1993.

ABSTRACT: Although geosynthetics are often used in soil reinforcement applications, there are currently no methods for estimating reliably the stresses within the reinforcements at working load levels. This paper summarizes the design of a new laboratory device, referred to as the Automated Plane Strain Reinforcement (APSR) cell, which measures the maximum tensile stress that develops at the center of a single planar inclusion due to shearing of the surrounding soil. The cell can accomodate a wide range of reinforcing materials and can be equiped with additional instrumentation to measure the distribution of strains and/or stresses with inclusions of half-lengths up to 450mm. Test data, obtained for an instrumented steel sheet inclusion embedded in Ticino sand, demonstrate the capabilities of the APSR cell for measuring load-transfer at working load levels. Simple closed form solutions based on shear lag analysis describe accurately the tensile stresses measured in the elastic steel sheet inclusion. The new device provides the capability to compare load-transfer characteristics for different classes of geosynthetic reinforcing materials.

KEYWORDS: New plane strain test, planar reinforcement, tensile stress measurement, shear lag analysis, sand-steel data.

INTRODUCTION

High strength polymer grids and strips, woven and non-woven fabrics are widely used to reinforce soil masses in the construction of retaining walls, embankments, foundations and pavements. The performance of these composite soil structures depends, in large part, on the interaction between the soil matrix and the inclusions which determines the magnitude of loads carried by the reinforcement. The mechanisms of interaction are particularly complex for reinforcements with non-planar

---

[1]Assistant Professor, Research Assistant, Principal Research Associate and Research Assistant, respectively, Massachusetts Institute of Technology, Cambridge, MA 02139.

surfaces, such as grids and for geosynthetic materials which exhibit non-linear and/or time dependent behavior. Existing analyses of soil-reinforcement interaction focus mainly on ultimate limit conditions using homogenization or limit equilibrium methods.

Homogenization methods [1] typically assume that the soil mass is reinforced with uniform, closely spaced inclusions and can be analyzed (at the macroscopic level) as an homogeneous, anisotropic composite material. Failure of composite reinforced soils has been investigated experimentally from measurements of boundary tractions and displacements in a variety of laboratory shear tests [2, 3]. These data show that the reinforcements produce an apparent cohesive strength component that is directly proportional to the density and strength of the inclusions. However, measurements in laboratory tests cannot be scaled reliably to field situations which are generally characterized by a relatively small number of reinforcing layers.

Current design methods for reinforced soil masses are generally based on limit equilibrium analyses [4] which postulate different mechanisms of failure and require input parameters to characterize the bond resistance between the soil and reinforcement in two modes: 1) direct shearing along the soil-reinforcement interface, and 2) tensile anchorage within the stable soil mass. These parameters are usually obtained from laboratory direct shear box (interface) and pullout tests, respectively. The measurements suffer from a number of well known practical limitations associated with poorly controlled test boundary conditions and are especially difficult to interpret for relatively extensible reinforcements (including many geosynthetics) and for inclusions with non-planar surfaces.

More comprehensive studies of soil-reinforcement interaction are necessary to understand the stress distribution within a reinforced soil mass at working load conditions. In principle, comprehensive stress analyses can be achieved using non-linear finite element (or boundary element) methods which model explicitly the constitutive properties of the soil, reinforcement and interfaces. Although these analyses offer great flexibility for simulating complex problem geometries, construction histories, etc., it is difficult to interpret the underlying mechanisms of soil-reinforcement interaction from complex numerical analyses. In contrast, this paper describes the development of a simple analytical framework for predicting and interpreting tensile stresses in a planar inclusion due to shearing of the surrounding soil. The analysis considers plane strain compression shearing of the soil mass with the inclusion oriented parallel to the minor, external principal stress. These studies provide the basis for the design of a new laboratory apparatus, referred to as the APSR cell, which is capable of measuring directly the tensile stresses within the reinforcement and imposes well defined boundary conditions on the soil specimen. Measurements in the APSR cell provide a method for comparing load-transfer characteristics for different types of geosynthetic reinforcements.

TENSILE STRESSES IN A PLANAR REINFORCEMENT

Figure 1 shows the idealized geometry for a composite plane strain element of reinforced soil which comprises a planar inclusion of thickness, f, and length, L, embedded in a soil matrix of overall height, m+f (corresponding to the typical inclusion spacing). The orientation of the inclusion is parallel to the minor, external, principal stress acting on the soil matrix, σ_3. The soil is sheared in a

plane strain compression mode by increasing the major principal stress, σ_1, at the boundary of the element (with σ_3 constant). For these loading conditions, the inclusion reduces the lateral tensile strains which would otherwise develop in the soil and hence, represents the optimal orientation for a planar tensile reinforcement. Abramento and Whittle [5] have adapted technqiues of 'shear lag' analyses, widely used in the mechanics of composites [6, 7, 8], in order to derive approximate analytical expressions for the tensile stresses in the reinforcement, σ^f_{xx}. Initially these analyses have assumed the following:

1. The soil matrix and reinforcement behave as linear, isotropic and elastic materials (with properties G_m, ν_m and E_f, ν_f, respectively, Fig. 1). It should be noted that deformation properties of the soil (and also some non-woven geosynthetic materials) are dependent on the confining stress level.
2. The soil matrix and reinforcing inclusion are linked through a frictional interface, described by an angle of interface friction, δ.
3. There is no axial stress acting at the ends of the reinforcement, (i.e. $\sigma^f_{xx}=0$ at $x=\pm L/2$) as the inclusion is thin and is not physically bonded to the soil matrix.

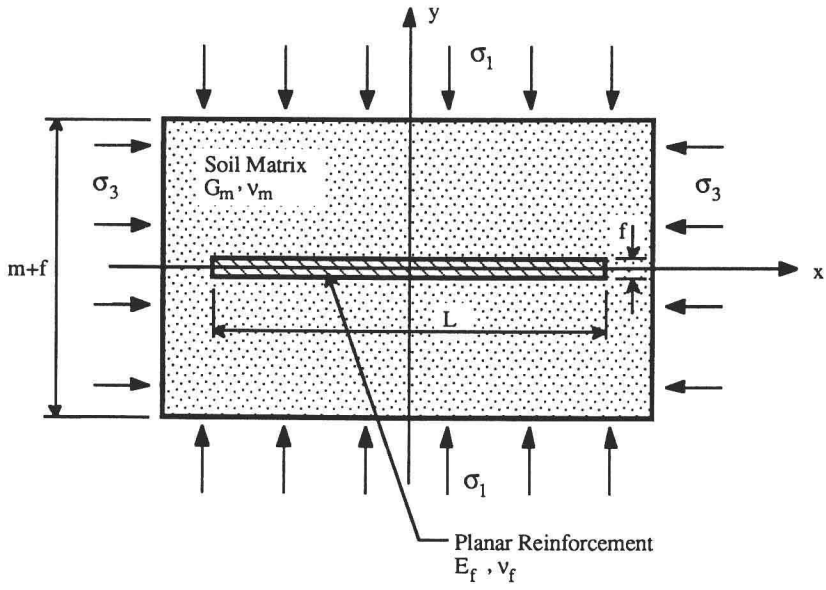

FIG. 1 Geometry of the reinforced soil element

For the case where there is no slippage at the soil-reinforcement interface, the tensile stress in the reinforcement can be written as a linear function of the external principal stresses σ_1 and σ_3:

$$\sigma^f_{xx} = \frac{K_2\,\sigma}{K_1}\left[\,1 - \frac{\cosh\sqrt{K_1}\;x}{\cosh\sqrt{K_1}\;\frac{L}{2}}\,\right] \qquad (1)$$

where,

$$K_2\,\sigma = K_2^1\sigma_1 + K_2^3\sigma_3 \tag{2}$$

and the coefficients K_1, K_2 can be written in terms of the elastic properties of the soil and reinforcement material, and the geometry (Fig. 1):

$$K_1 = \frac{6}{m\,f}\,\frac{\left[\left(1-\nu_m\right)a + 2\,\frac{G_m}{E_f}\left(1+\nu_f\right)\left(1-\nu_f\right)\right]}{\left[1+\frac{1}{4}\nu_m - \frac{3}{2}\,\frac{G_m}{E_f}\left(1+\nu_f\right)\nu_f\right]} \tag{2a}$$

$$K_2^1 = \frac{6}{m\,f}\,\frac{\left[\nu_m - 2\,\frac{G_m}{E_f}\left(1+\nu_f\right)\nu_f\right]}{\left[1+\frac{1}{4}\nu_m - \frac{3}{2}\,\frac{G_m}{E_f}\left(1+\nu_f\right)\nu_f\right]} \tag{2b}$$

$$K_2^3 = -\frac{6}{m\,f}\,\frac{\left(1-\nu_m\right)\left(1+a\right)}{\left[1+\frac{1}{4}\nu_m - \frac{3}{2}\,\frac{G_m}{E_f}\left(1+\nu_f\right)\nu_f\right]} \tag{2c}$$

where a=f/m.

The accuracy of these expressions has been established through comparisons with numerical results from finite element analyses [5].

It is clear from equation 1 that the maximum tensile stress occurs at the center of the inclusion (i.e., σ^f_{max} occurs at x=0) and that the maximum stress in a long reinforcement (i.e., typical of the field situation) is given by:

$$\sigma^f_\infty = \left(\sigma^f_{xx}\right)_{L=\infty} = \frac{K_2\sigma}{K_1} \tag{3}$$

This result shows that the maximum tensile stress in a long inclusion is controlled by three factors: 1) the shear stress mobilized in the soil matrix, σ_1/σ_3; 2) the relative stiffness of the inclusion

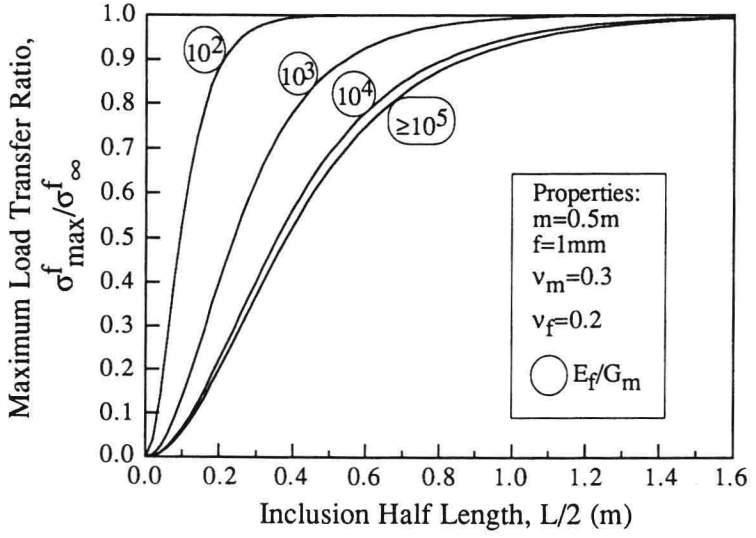

FIG. 2 Effect of inclusion length and stiffness on maximum load transfer ratio

and soil, E_f/G_m; and 3) the volume ratio of the reinforcement, a=f/m.

Figure 2 summarizes the 'maximum load transfer ratio', $\sigma^f_{max}/\sigma^f_\infty$ as a function of the inclusion half-length, L/2, and the stiffness ratio, E_f/G_m, for an inclusion with typical thickness, f=1mm, and spacing, m=0.5m. The results show that the 'pick-up length' necessary to achieve maximum load transfer (i.e., $\sigma^f_{max} \Rightarrow \sigma^f_\infty$) increases significantly with the stiffness ratio. For a relatively inextensible reinforcement such as steel ($E_f/G_m \approx 10^4$, Fig. 2), the maximum load transfer occurs for inclusions with half-lengths $L/2 \geq 1.5$m; while more extensible materials ($E_f/G_m=10^2$, Fig. 2) achieve similar conditions for $L/2 \approx 0.4$m. These results have important implications on the measurements of load transfer in small scale laboratory tests and in the application of these data for predicting field performance.

Figure 3 illustrates the distribution of the tensile stress, σ^f_{xx}, normalized by the major principal stress, σ_1, for typical material properties, spacing and thickness of the reinforcement (Fig. 3). The results for inclusions with half-lengths, L/2=0.25, 0.5 and 1.5m, at an external stress ratio, $\sigma_1/\sigma_3=6$ (Fig. 3a), show that there are two distinct regions which characterize the soil-reinforcement interaction: I) the zone close to the tip of the inclusion, in which the tensile stress accumulates due to shear stresses acting along the soil-reinforcement interface and II) the zone of constant axial inclusion stress (i.e., $\sigma^f_{xx} \Rightarrow \sigma^f_\infty$). These two regions are fully developed for 'long' inclusions (e.g., L/2=1.5m; Fig.3a). For 'short' inclusions (L/2=0.25, 0.5m; Fig.3), the maximum load transfer is not achieved, and the shear lag parameter, K_1 (Eqn. 2a) controls the distribution of tensile stresses in zone I.

Figure 3b shows the load transfer for a short inclusion with half-length, L/2=0.5m, as a function of the applied stress ratio, σ_1/σ_3 in the soil matrix. For a soil matrix with linear, isotropic properties, the ratio $\sigma_1/\sigma_3 = (1-\nu_m)/\nu_m = 1/K_0$ (i.e., for $\nu_m=0.3$, $1/K_0 = 2.3$; Fig.

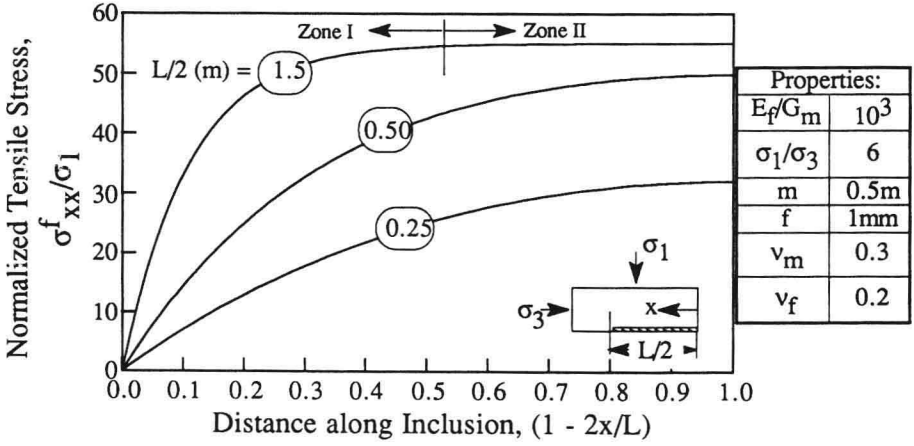

a) Effect of inclusion length

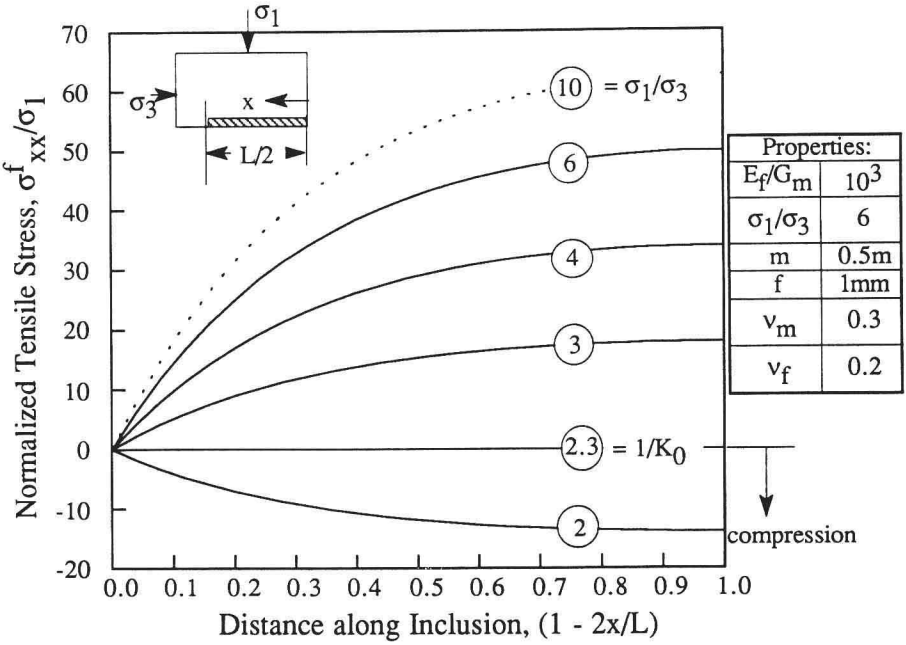

b) Load transfer due to shearing of the soil

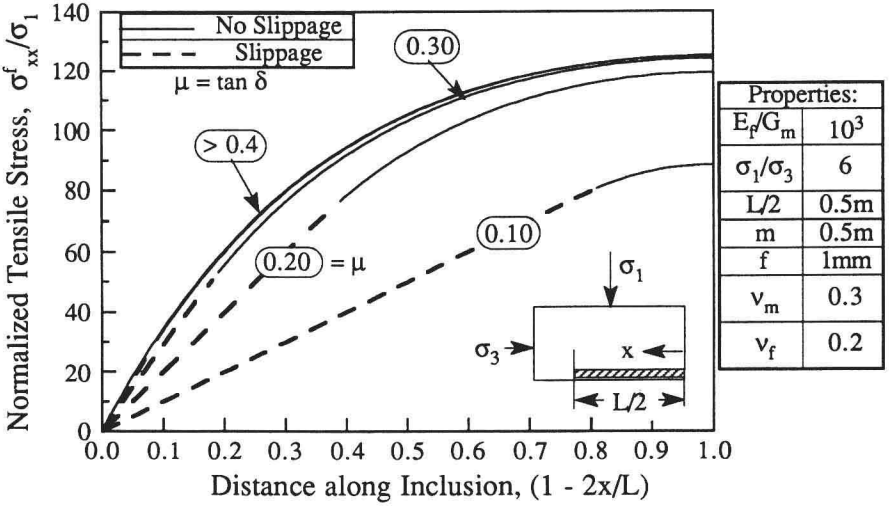

c) Effects of interface friction

FIG. 3 Distribution of tensile stresses in a planar reinforcement

3b) corresponds to one-dimensional deformation of the unreinforced soil matrix (i.e., $\varepsilon_{xx} = 0$). Tensile stresses only develop in the reinforcement when $\sigma_1/\sigma_3 > 1/K_0$. There are two important limitations on the interpretation of results in Figure 3b:

1. For drained shearing of dry, cohesionless soils (e.g. good quality granular fills), the shear strength is most commonly described by a Mohr-Coulomb failure criterion with friction angle $\sin \phi = (\sigma_1-\sigma_3)/(\sigma_1+\sigma_3)$. Ladd et al. [9] report $35^0 \leq \phi_{ps} \leq 57^0$ ($3.7 \leq \sigma_1/\sigma_3 \leq 11.7$) for typical sands sheared in plane strain compression. Thus, local failure will initiate in the matrix (at locations close to the tip of the inclusion) when the stress ratio mobilizes the frictional strength of the soil.
2. The linear, isotropic model of soil behavior does not describe accurately the volumetric response of cohesionless soils in drained shearing at high stress ratios. Extensive observations show that sands dilate when the mobilized friction exceeds a threshold value, $\phi_{cv} = 35^0$ to 45^0 ($\sigma_1/\sigma_3 = 3.7$ to 5.8) [10, 11]. The practical implication of this behavior is that the proposed analysis will tend to underestimate both the lateral strains in the soil matrix and the tensile stresses in the reinforcement (especially for $\sigma_1/\sigma_3 > 6$).

The preceding results assume that there is no slip between the soil matrix and the planar reinforcement. The results in Figure 3c show the effects of the interface friction angle, δ, on the load transfer for an inclusion of half-length, L/2=0.5m, at a stress ratio, σ_1/σ_3=6. For the selected material properties and geometry, interface slippage has very little influence on tensile stresses in the reinforcement for $\delta \geq 17^0$ ($\mu = \tan \delta \geq 0.3$). However, there are significant reductions in load transfer when the friction ratio is artificially low (μ=0.1, $\delta=7^0$). Further studies [5] also show that, for practical values of interface friction, $\delta=10^0$-30^0, interface slippage has little effect on the expected load transfer for a wide range of constituent material properties and inclusion geometries.

THE APSR CELL

The analysis summarized in the previous section provides a framework for predicting and interpreting the load transfer for the unit element geometry shown in Figure 1. The framework also provides the basis for the design of a new laboratory device, referred to as the Automated Plane Strain Reinforcement (APSR) cell, for measuring the maximum tensile stress transferred to a planar reinforcement due to plane strain shearing of the surrounding soil [11]. The boundary conditions along the plane of symmetry, x=0, in the unit element (Fig. 1) are well defined by 1) zero lateral displacement in both the soil and reinforcement (i.e., u_x=0), 2) no shear tractions acting along the plane (i.e., σ_{xy}=0). These conditions are simulated in the design of the APSR cell (Fig. 4) which corresponds to one-half of the unit element containing an inclusion of length, L/2. The rear wall of the cell is rigid and lubricated to minimize friction along the centerplane of the unit element. The key design feature of the APSR cell is that the inclusion is clamped externally to a load cell which measures the force in the reinforcement at a location equivalent to the centerline of an inclusion with length, L. In order to maintain the symmetry along the rear wall, an hydraulic piston controls the position of the reinforcement such that there is no displacement of the inclusion at the reference entry point, marked **X** in Figure 4.

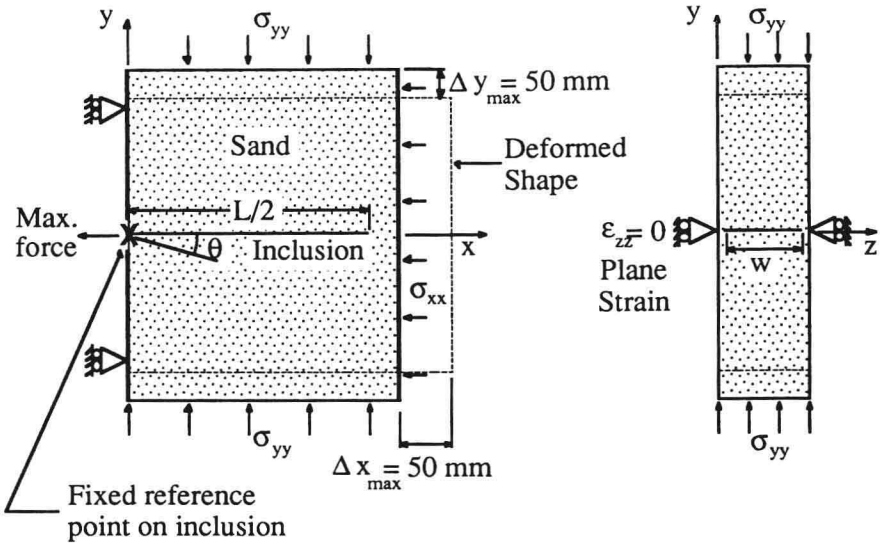

FIG. 4 Schematic diagram of the APSR cell

Figure 5 shows the actual cross-section through the APSR cell. It contains a soil specimen of overall dimensions 570mm high by 450mm wide by 150mm deep (plane strain direction), which is enclosed by a thin rubber membrane. The reinforcing inclusion, with half-length up to L/2=450mm, passes through a slot in the rear wall of the cell and is supported by jacking against an external support arch. The entry slot can be custom designed for inclusions up to 10mm thick. The cell applies air pressure to the outside of the specimen to control the confining stress ($\sigma_3 \leq 50$kPa), while the major principal stress is imposed through two loading platforms via waterbags which provide uniform boundary tractions. The device can impose relatively large axial strains (up to 10%), which are necessary for investigating load transfer using extensible reinforcements [12], while the specimen is free to deform laterally into the air void at the front of the cell. The plane strain walls of the APSR cell have an unique active control system which ensures that the lateral strains, $\varepsilon_{zz} \leq 0.01\%$ throughout the test.

The following paragraphs summarize the principal design features of the APSR cell [11]:

1. The length of the reinforcing inclusion is an important factor in selecting the dimensions for the APSR cell. Shear lag analyses show that maximum load transfer, corresponding to prototype field conditions can be achieved for inclusions with half-lengths, L/2=1.0 to 2.0m (cf. Fig. 2). These dimensions cannot readily be achieved in a laboratory test. Instead, the dimensions of the APSR cell have been selected to handle commercially available reinforcing materials including typical geogrids.

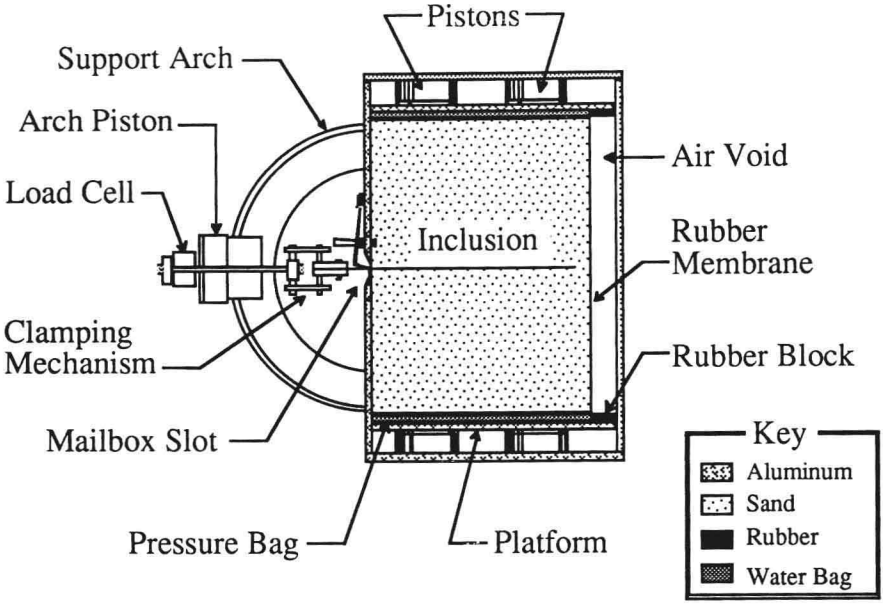

FIG. 5 Section through the APSR cell

Measurements of load transfer obtained for inclusions of different lengths then provide the basis for evaluating tensile stresses at prototype scale.

2. The magnitudes of the applied boundary tractions determine the structural (strong box) design of the APSR cell. The device can apply a major principal stress, $\sigma_1 \leq 500$kPa (Fig. 4) through two water bags mounted on moveable rigid platforms. Uniform lateral confinement, $\sigma_3 \leq 50$kPa is provided by air pressure acting on the rubber membrane which encloses the soil specimen. All contact surfaces are lubricated with a 50-50 mixture of high vacuum silicon grease and a release agent in order to minimize friction in the system.
3. The cell can impose axial strains of up to 10% on the specimen which are sufficient to cause failure of unreinforced sand specimens and to develop maximum load transfer even for relatively extensible geosynthetic reinforcements. Plane strain conditions are achieved through an active system using a pressurized water diaphragm within the side walls. This novel design reduces significantly the size of the walls that would otherwise be required, and enables remote measurement of the displacements within the specimen using radiography. Radiographic measurements provide a method for establishing the uniformity of strains in the unreinforced soil specimen and can also monitor the mechanisms of soil-reinforcement interaction.
4. The APSR cell is fully automated and includes eight independent, closed, feedback control loops for the displacements of the drive pistons, lateral diaphragm walls, arch support jack and confining air pressure. These are controlled by a single microcomputer and three custom-built, analog feedback circuits. Automation provides great flexibility in test procedures and enables soil specimens to be sheared under conditions of stress or displacement control. These

capabilities are particularly useful in measuring load transfer for geosynthetic reinforcements which exhibit significant time dependent properties. Instrumentation for the control of boundary tractions and displacements includes: a) a proximity sensor to monitor the reference position, **X** (Fig. 4); b) pressure transducers, which measure the hydraulic pressure in the water bags and the confining air pressure; c) displacement transducers, which monitor and control the movement of the platforms and side walls; and d) additional displacement transducers which measure directly the axial and lateral deformations of the specimen.

5. Sand specimens are prepared by raining particles through an assembly of sieves (dry pluviation) in order to achieve specimens of specified target densities which are homogeneous and exhibit repeatable engineering properties. The raining apparatus for the APSR cell comprises a sand hopper with a perforated base mounted on a 1.4m high chimney which contains a series of wire mesh screens. The depositional process also introduces a structure or fabric such that the mechanical properties of the sand are cross-anisotropic. The APSR cell is designed such that the specimen can be deposited along either the z or y axes (Fig. 4). Sand specimens deposited in the z direction initially exhibit isotropic properties for plane strain shearing in the x-y plane, while those formed in the y-direction have cross-anisotropic properties. This important design feature decouples the effects of soil anisotropy in the measurements of load transfer using the APSR cell.
6. The external load cell measures the maximum tensile force in the reinforcement at the reference location **X** (Fig. 4). Additional instrumentation can be designed to measure local strains and/or stresses at locations along the inclusion for different types of reinforcing material. Deformations within the soil specimen are computed from radiographic measurements of the displacements of tungsten-steel markers embedded in the soil [13].

Larson [11] describes the extensive program of proof tests which have been performed to evaluate the design and performance of the APSR cell. The tests are all performed using dry Ticino sand as the reference soil. The physical and engineering properties of Ticino sand are typical of many natural sands and are well documented in the literature [14]. The sand is deposited along the z-axis of the APSR cell (Fig. 4) with initial relative densities, $D_r \approx 30$ and 75% (loose and dense specimens, respectively). The proof tests have: a) established that the silicon grease lubrication is successful in minimizing wall friction in the APSR cell; and b) refined test procedures such that measurements of stress-strain behavior (for the unreinforced sand) and load transfer for elastic inclusions are repeatable and consistent. The stress-strain-strength properties of the unreinforced Ticino sand, measured in the APSR cell, are in good agreement with results from other plane strain devices reported in the literature [9].

MEASUREMENTS OF LOAD TRANSFER FOR A STEEL SHEET INCLUSION

A comprehensive reference program of load transfer measurements have been obtained in the APSR cell using dense and loose Ticino sand reinforced with two-ply, elastic steel sheet inclusions [11]. All of the tests were performed at a confining stress σ_3=31kPa and include local measurements of the strain distribution within the reinforcement from a series of uniformly spaced, bonded resistance strain gauges which are sandwiched between the two thin steel sheets (each 0.13mm thick).